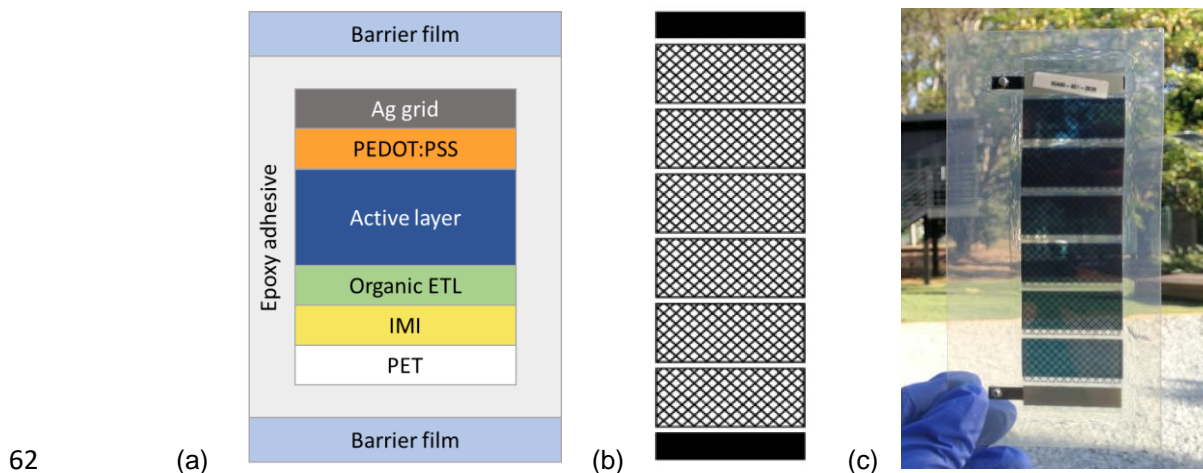


46 (P3HT) and the fullerene phenyl-C61-butyric acid methyl ester (PCBM). In this work, two different OPV
47 materials have been tested outdoors at operational conditions in two different locations (Belo Horizonte
48 in Brazil and Bangor, Wales) in order to compare the stability at both locations.

49 2. EXPERIMENTAL

50 2.1 Sample preparation

51 The OPV devices used in this study were manufactured by CSEM Brasil following the inverted structure,
52 as depicted in Figure 1. The modules were processed in a single station roll-to-roll (R2R) machine
53 (Smart Coater SC09 from Coatema Coating Machinery GmbH, modified by CSEM Brasil) on a flexible
54 substrate sputtered with indium tin oxide/metal/indium tin oxide (IMI), supplied by Oike, using non-
55 chlorinated solvents. All layers were processed in air. A standard amine based polymer was used as
56 electron transport layer (ETL) and polyethylenedioxythiophene:polystyrenesulfonate (PEDOT:PSS) as
57 hole transport layer (HTL). Two blue commercial active layer formulations by Merck were tested, referred
58 as first and second-generation (Gen-I and Gen-II respectively). Both inks are fullerene-derivatives based
59 and differ in donor due to a small change in the Gen-II co-polymer for improved light stability. The six
60 coated strips were serially connected by a silver top electrode 80% rich in Ag deposited via a flatbed
61 semi-automatic screen printer, resulting in modules with 6 cells and total active area of 21.6cm².



62 (a) (b) (c)
63 **Figure 1** - Schematics of (a) individual layers and (b) the six cells connected as a module. (c) Encapsulated sample.

64 The samples were further encapsulated with a multilayer of PET-based barrier film with a water vapor
65 transmission rate (WVTR) in the order of $10^{-3} \text{ gcm}^{-2}\text{day}^{-1}$ from Mitsubishi, using a Delo epoxy-based UV-
66 curable adhesive with barrier properties ($6 \text{ gcm}^{-2}\text{day}^{-1}$), in a R2R lamination machine, built in house,
67 which uses a nip pressure to reach a thin and homogeneous layer of glue of approximately $40 \mu\text{m}$. The
68 performance of the modules was first evaluated at CSEM Brasil under an AAA solar simulator, Wacom
69 WXS-156S-10, AM 1.5G, with illumination of $1,000 \text{ W m}^{-2}$. Electrical parameters of the selected devices
70 after encapsulation were: short-circuit current density, $J_{\text{SC}} = (8.87 \pm 0.09) \text{ mA cm}^{-2}$, open-circuit voltage,
71 $V_{\text{OC}} = (5.02 \pm 0.03) \text{ V}$, fill factor, $\text{FF} = (54 \pm 3) \%$ and power conversion efficiency, $\text{PCE} = (4.0 \pm 0.2) \%$,
72 for Gen-I modules, and $J_{\text{SC}} = (9.4 \pm 0.2) \text{ mAcm}^{-2}$, $V_{\text{OC}} = (5.11 \pm 0.02) \text{ V}$, $\text{FF} = (57.0 \pm 0.4) \%$ and $\text{PCE} =$
73 $(4.56 \pm 0.07) \%$ for Gen-II. These results are averaged from 6 devices of each generation. In order to
74 avoid any problems during the shipment, such as light degradation or mechanical stress, the samples
75 were sent to Bangor in nitrogen bags, protected from humidity and light exposure, and sandwiched
76 between rigid plates.

77 2.2 Outdoor test

78 The samples were subjected to the outdoor test in two different sites, Belo Horizonte (BH), Brazil (19.9°
79 S, 43.9° W) and Bangor, Wales (53.2° N, 4.1° W), following the protocol of ISOS-O-2¹⁷ and using local

80 existing testing installations and measurement systems. In both locations, the tilt angles were chosen
81 as the optimum fixed tilt angle considering yearly generation ²⁷.

82 3 modules were tested in Belo Horizonte, exposed to outdoor conditions on a rooftop on a rack facing
83 North at an angle of 20° and connected to a measurement system that uses relay plates and a
84 multiplexer. Current-Voltages (I-V) curves of each sample were taken automatically every hour and,
85 when not under measurement, the modules were connected to resistive loads in order to operate close
86 to the maximum power point (MPP). Weather data was collected with a weather station and the
87 irradiance values were taken with a pyranometer (Solys 2 from Kip & Zonnen), tilted at the same angle.
88 In this system, irradiance measurements were taken before and after each I-V curve in order to exclude
89 data collected when there was important irradiance change, such as when clouds passed.

90 In Bangor, 2 modules were tested, orientated southwards at an inclination angle of 35°, also biased at
91 MPP, with IV measurements every 10 minutes. Weather parameters were collected using a Davis
92 weather station Vantage Pro and irradiance data was collected using calibrated silicon solar cells and a
93 pyranometer, tilted at the same angle. Pictures of the setups are shown in Figure 2.

94 (a)



(b)



95
96 **Figure 2** - Outdoor monitoring setup used to perform the tests in (a) Belo Horizonte, Brazil, at an angle of 20°, facing
97 North, and (b) Bangor, Wales, with an inclination of 35°, facing South. The already existing installations and
98 measuring systems were used.

99 **2.3 Data analysis**

100 The data was analyzed, based on the rules: (i) only using data points collected between 7:00 and 18:00;
101 (ii) a range of 5% for each selected irradiance, i.e., $(300 \pm 15) \text{ W m}^{-2}$; (iii) exclusion of data points differing
102 up to 30% from adjacent measurements, to eliminate measurement errors due to equipment failure or
103 the effect of clouds/moving shades; (iv) in the case of Belo Horizonte, exclusion of data points where
104 the irradiance measurements before and after each I-V curve differed more than 5%.

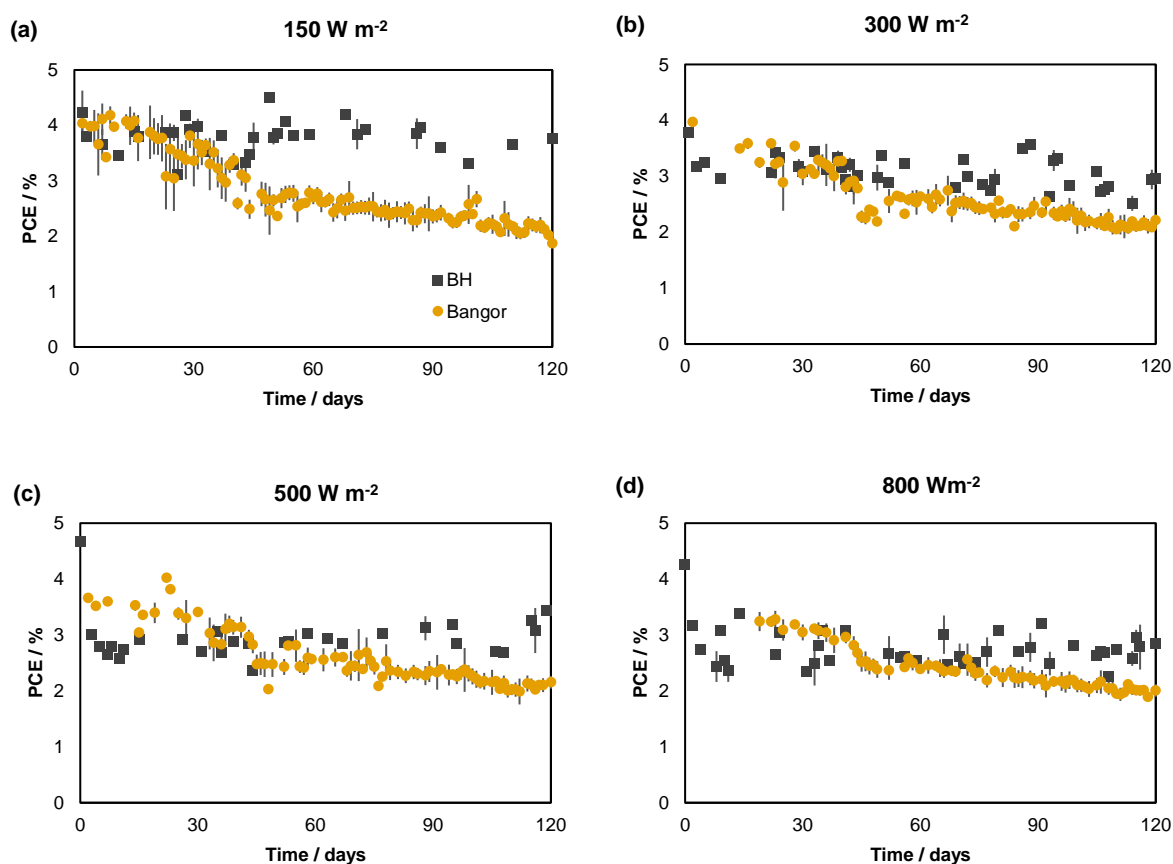
105

106 **3. RESULTS AND DISCUSSION**

107 **3.1 Gen-I modules**

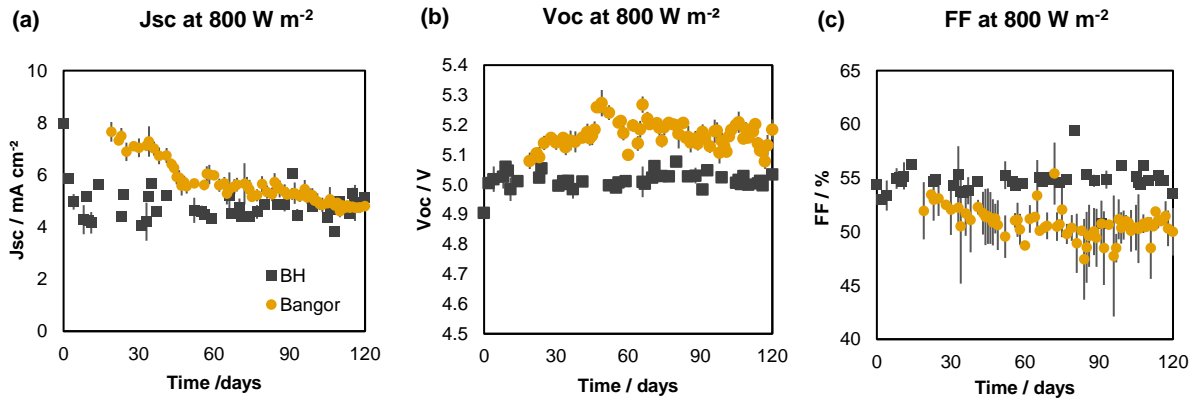
108 Figure 3 (a-d) shows how the performance of the modules fabricated with the first-generation ink
109 changed over time. The test was initialized in January 2018, which corresponds to winter in Bangor and
110 summer in Belo Horizonte. Despite the lower irradiance levels in the winter season, modules in Bangor
111 exhibited a higher degradation than those in Belo Horizonte (BH). For the test conducted in Bangor, the

112 curve is clearly divided in two linear segments, the first one, up to 50 days, showing a steeper slope.
 113 Considering the data in Figure 4, this seems to be connected with J_{SC} . The other electrical parameters,
 114 V_{OC} and FF, exhibited less relative variation with a minor increase in V_{OC} which is offset by a moderate
 115 reduction in FF. By contrast, modules deployed in Belo Horizonte show an exponential decrease in the
 116 first days, what is commonly called in the literature as *burn-in*²⁰, and a steady performance afterwards.
 117 The parameter that shows the greatest relative change was J_{SC} , which is usually attributed to the
 118 photoinduced dimerization of the fullerene acceptor^{28,29}; FF and V_{OC} remained approximately constant.
 119 By analyzing the plots under different irradiance levels, it could be seen that the general shape of the
 120 degradation curves pattern is the same, although BH modules show higher PCE values under 150 W
 121 m^{-2} , which could be attributed to measurements on cloudy days and spectral mismatch. This difference
 122 was not as pronounced in Bangor. In either case, there was no visual sign of delamination or corrosion
 123 of the contacts.



124

125
 126 **Figure 3** - Performance over time for Gen-I modules tested in Belo Horizonte and Bangor, measured at the
 127 irradiance of (a) 150 W m^{-2} , (b) 300 W m^{-2} , (c) 500 W m^{-2} and (d) 800 W m^{-2} . The test was started in January 2018.
 128 Error bars represent the standard deviation.

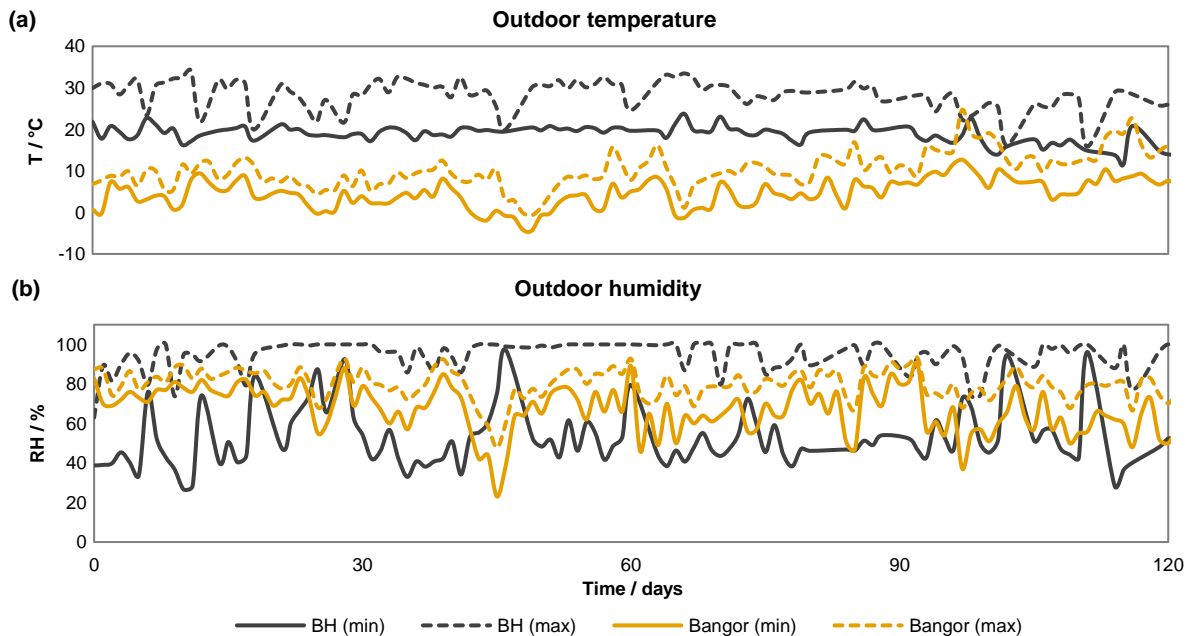


129

130 **Figure 4** - Evolution of the electrical parameters of Gen-I modules at 800 W m^{-2} : (a) J_{sc} , (b) V_{oc} and (c) FF. Error
 131 bars represent the standard deviation.

132 In Bangor, the measured drop of J_{sc} is lower than in BH in the first days of testing, which is consistent
 133 with the lower level of irradiance in January in that region. The energy dose delivered in the period was
 134 1025 MJ m^{-2} in Bangor, against 1837 MJ m^{-2} in Belo Horizonte. The lifetime of the modules was
 135 estimated based on a linear regression as the time to reach 80% of the efficiency after the burn-in (T80).
 136 In Belo Horizonte, Gen-I modules were expected to last 180 days, with a burn-in of 30%, while in Bangor,
 137 T80 was reached after 50 days.

138 The additional weather data collected during this period is shown in Figure 5. The change in slope
 139 observed for the modules in Bangor coincides with the period of increasing temperature. In Belo
 140 Horizonte, there was no significant change up to 90 days, when the temperature drops slightly. Overall,
 141 the temperature in Belo Horizonte was higher in Bangor, but the averaged relative humidity was similar
 142 (although the amplitude was significantly higher). These environmental conditions seemed at odds with
 143 the faster degradation observed in Bangor, which is discussed in more detail later.



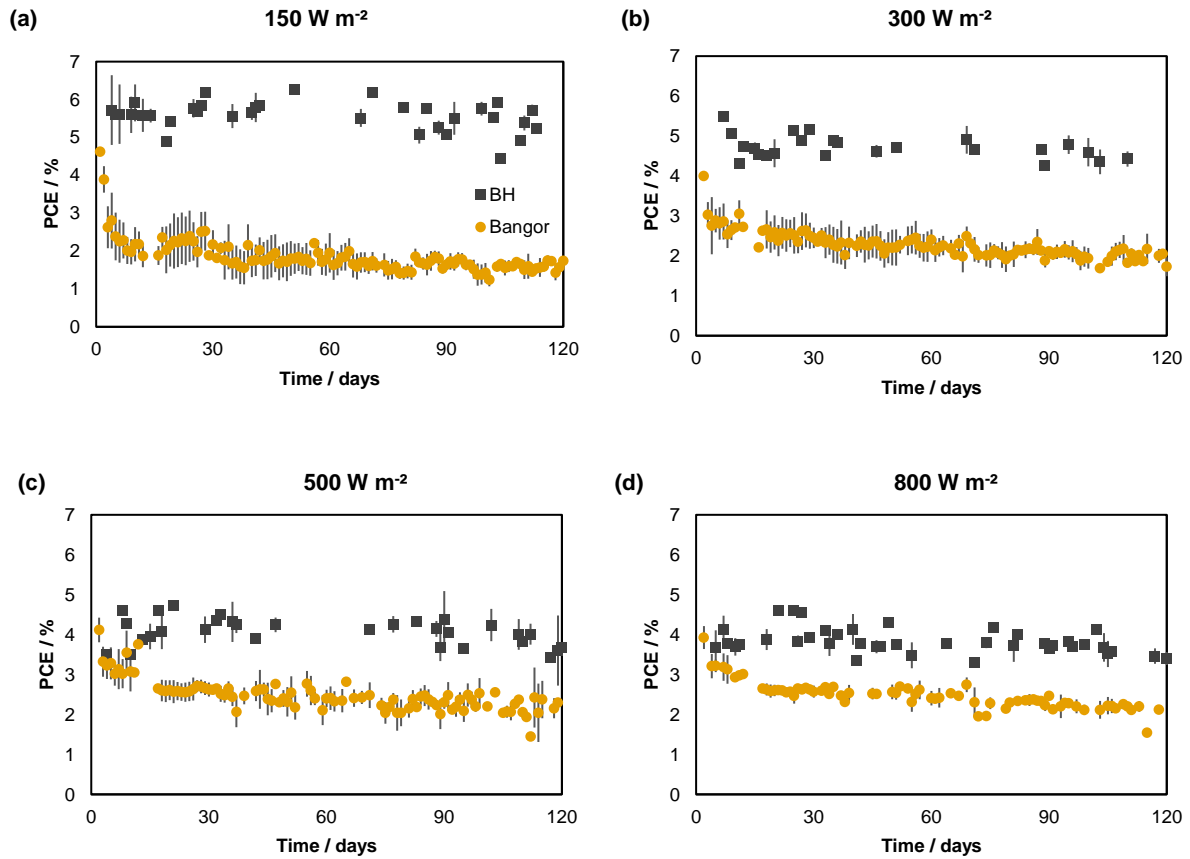
144

145 **Figure 5** - Weather conditions during the first campaign, with maximum and minimum daily values of (a) temperature
 146 and (b) humidity.
 147

148 **3.2 Gen-II modules**

149 A second generation of modules was tested using the same experimental procedure and number of
150 modules as the previous test. Gen-II is a modified ink that aimed at better light stability, which was
151 confirmed in indoor tests. Monitoring started in early Autumn in Belo Horizonte and Spring in Bangor
152 and the PCE results are shown in Figure 6. As with the first campaign, Gen-II modules also exhibited a
153 faster degradation in Bangor, but, in this case, the curve had a different shape: a high burn-in was noted,
154 resulting in a ~ 25% loss in PCE, followed by a linear degradation thereafter. Comparing the different
155 light levels, the degradation curve was very similar, although at 150W/m² the first data point depicts a
156 higher PCE. This would result in a higher burn-in, but there is no evidence that modules would present
157 a different pattern of degradation at different light levels; thus it is possible that the first measurement is
158 not accurate, and could be a result of shading on the pyranometer at that moment of the IV tracing. In
159 Belo Horizonte, the burn-in could not be easily seen, since the first data days were cloudy. However,
160 considering that samples had very similar initial parameters, it is likely that these modules did not
161 experience a high initial degradation and were, thus, more stable in Belo Horizonte. By considering the
162 electrical parameters, shown in Figure 7, it can be seen that J_{sc} values decreased at a similar rate at
163 both sites, whilst the V_{oc} and FF dropped at a greater rate in Bangor. A drop in V_{oc} is usually seen
164 when there is water penetration on the samples, which also causes an increase in series resistance and
165 reduction of FF. Water is absorbed by the hydrophilic PEDOT:PSS HTL and increases the resistivity
166 and modifies the HTL/phot-active layer interface, which can ultimately lead to delamination of the
167 layers^{19,30}. Data on series and shunt resistance are included in the Supplementary Information.

168 During the second campaign, the differences in the weather conditions were not as large as in
169 the first case, as shown in Figure 8. However, the temperature and maximum levels of relative humidity
170 daily values, as well as the energy dose, were higher in Belo Horizonte: 1800 MJ m⁻² against 1505 MJ
171 m⁻² in Bangor. As with Gen-I modules, it is clear that the elevated ambient parameters in BH do not
172 seem to increase the degradation rate of the OPV modules. The estimated lifetime for the modules in
173 Belo Horizonte, was 279 days, against 90 days for modules in Bangor, considered after the burn-in of
174 approximately 25%.

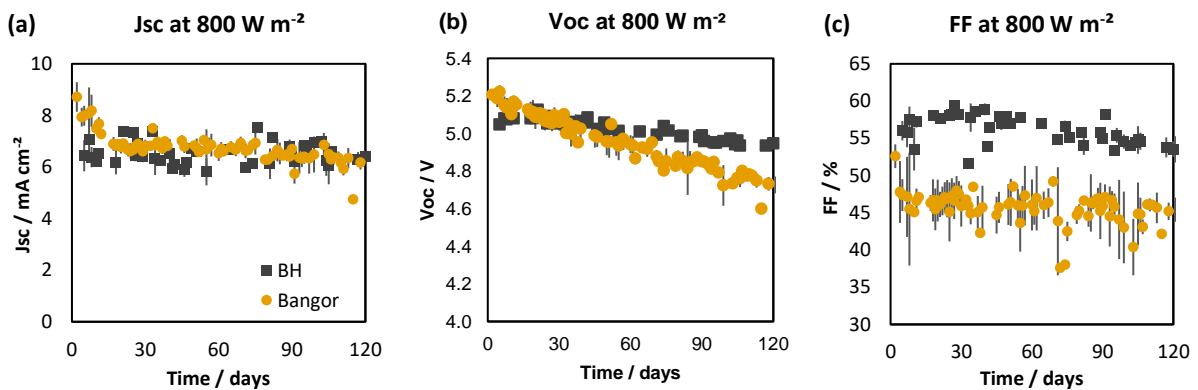


175

176

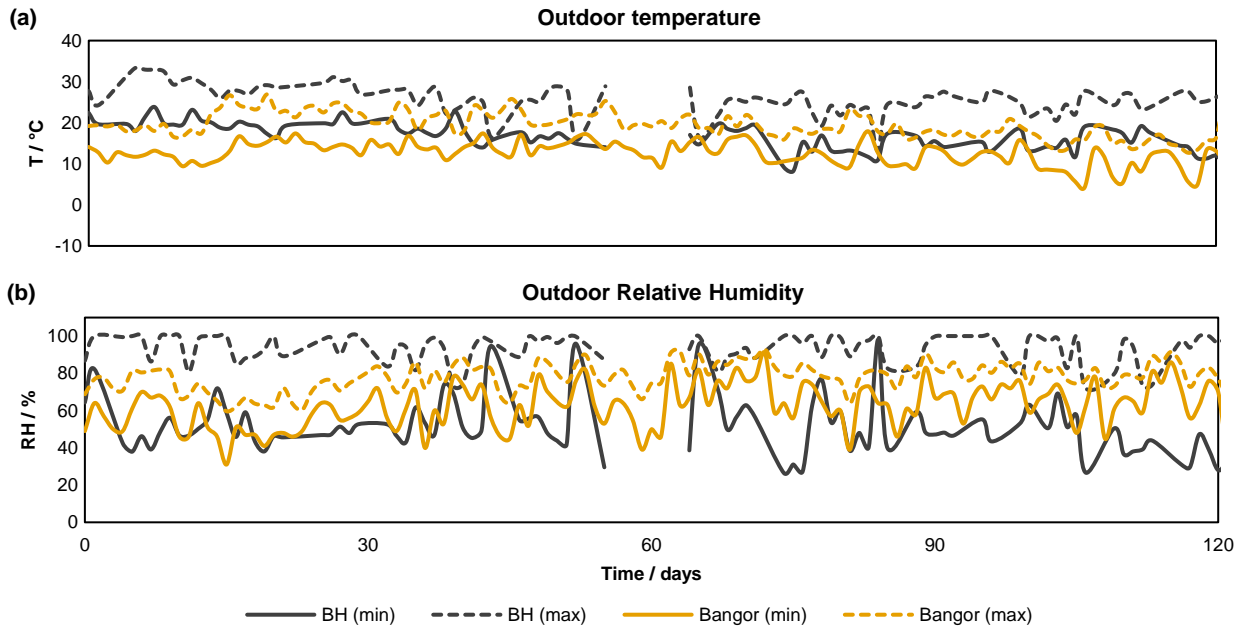
177 **Figure 6** - Performance over time for Gen-II modules tested in Belo Horizonte and Bangor, measured at the
 178 irradiance of (a) 150 W m^{-2} , (b) 300 W m^{-2} , (c) 500 W m^{-2} and (d) 800 W m^{-2} . The test was started in May 2018.
 179 Error bars represent the standard deviation.

180



181

182 **Figure 7** - Evolution of the electrical parameters of Gen-II modules at 800 W m^{-2} (a) J_{sc} , (b) V_{oc} and (c) FF. Error
 183 bars represent the standard deviation.



184

185

186

187

Figure 8 - Weather conditions during the second campaign, with maximum and minimum daily values of (a) temperature and (b) humidity.

188

189

190

191

192

193

194

195

196

Given that both sites used the same modules from the same production run, the reasons for the variation in stability are limited. Differences in light spectra between the locations could possibly explain the different burn-in values observed. Potentially transportation could also induce some mechanical issues. Furthermore, the measurement system in Bangor is located around 400m east of the Menai straits, so salinity is likely to be higher (although prevailing winds come from the west). This could be a contributing factor to the greater degradation observed in Bangor, but the increased levels of condensation on modules in Bangor could also be an issue. Condensation could induce a number of failure mechanisms, such as weakening of barrier layers and the adhesive, absorption of water into the modules as well as higher levels of localized relative humidity.

197

198

199

200

201

202

Although more rainy days were observed in Belo Horizonte, the daily amplitude of relative humidity was similar to Bangor, but the minimum levels of relative humidity were often much lower than Bangor as a result of the higher temperatures in BH. In Bangor, the maximum and minimum values of relative humidity were very close and constantly high. Combined with low temperature, especially during the first campaign, this could indicate higher condensation, which could have had a significant impact on the module degradation.

203

3.3 Condensation effect

204

205

To evaluate the impact of condensation on the results, the dew point temperature was approximated using the Magnus-Tetens equation:

206

$$T_d = \frac{b \times \alpha(T, RH)}{a - \alpha(T, RH)}$$

207

and

208

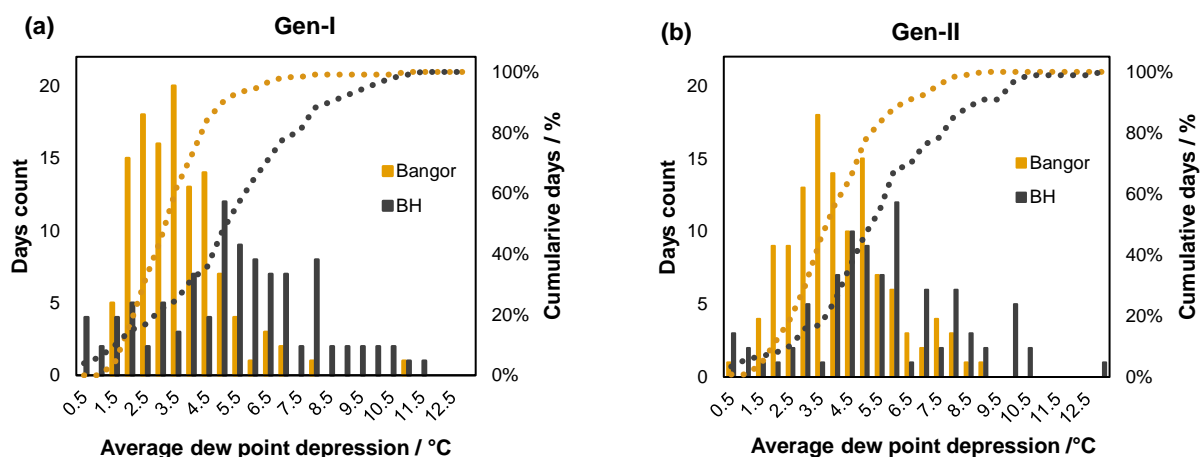
$$\alpha(T, RH) = \ln \frac{RH}{100} + a \times \frac{T}{b + T}$$

209

210

where T_d is the dew point temperature; T is the temperature; RH is the relative humidity of the air; a and b are coefficients. For Sonntag90 constant set, $a = 17.62$ and $b = 243.12$ °C^{31,32}. One way to evaluate

211 the level of condensation at both sites is to consider the average dew point depression (DPD), i.e., the
 212 difference between the ambient temperature and the dew point temperature, which was calculated for
 213 each day of testing at both locations. Figure 9 presents this data in a histogram. The graphs show that,
 214 in both periods, the average dew point depression in 50% of the days analyzed was lower than 3.5 °C
 215 in Bangor, against 5.5 °C in Belo Horizonte. When raised to 80%, the numbers change to 5.5 °C and
 216 7.9 °C, respectively. As there are more hours when the ambient (and hence module) temperature is
 217 closer to the dew point in Bangor, it can be deduced that condensation levels in Bangor were higher
 218 than in Belo Horizonte, which could have increased the water penetration through the encapsulation.



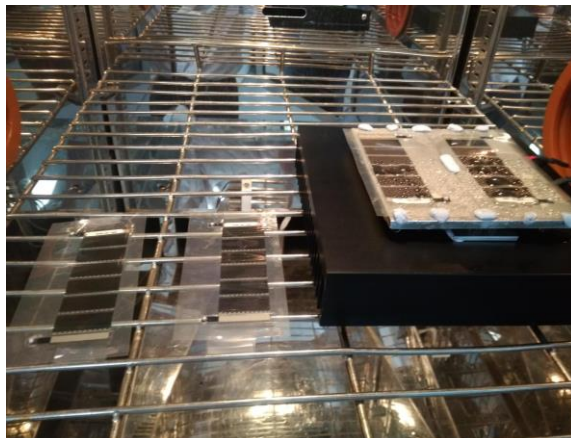
219
 220 **Figure 9** - Histogram of the average daily dew point depression for the periods of (a) Gen-I and (b) Gen-II
 221 monitoring.

222 Condensation is rarely studied in the context of PV degradation, possibility because this is unlikely to
 223 be a major issue in crystalline silicon modules given the use of glass as encapsulant material. However,
 224 flexible OPVs are encapsulated with polymeric films that are prone to water penetration, which can
 225 degrade contacts, transport and active layers^{20,22}. Therefore, special attention is required in this case.

226 An experiment ran in Bangor with a different low band-gap polymer and fullerene acceptor formulation
 227 shows the effect of condensation on the degradation of OPV modules. The test was performed with six
 228 identical modules inside a climate chamber with a controlled environment, following the ISOS-D-3
 229 standard, where the temperature and relative humidity (RH) of the chamber were set to 65°C and 85%
 230 respectively, as shown in Figure 11 (a). Two modules were tested at these standard conditions, whilst
 231 four other modules were placed on Peltier cooling devices, which lowered the modules' temperature to
 232 60 °C and 57 °C, as depicted in Figure 10 (two modules at each temperature condition). By lowering the
 233 temperature, water drops were allowed to form on the surface of the modules simulating the outdoor
 234 condensation. As the dew point at 65 °C is 61.4 °C, the temperature conditions tested corresponded to
 235 a dew point depression of 3.6°C for the control sample and -1.4 and -4.4 °C for the cooled samples,
 236 respectively. In practice, a negative dew point is unlikely to occur in operation, but it is a common effect
 237 at night, particularly in cold regions with high relative humidity, such as continental and northern Europe.
 238 At night, the panel releases heat into the atmosphere by radiation and if its temperature falls below the
 239 dew point, water condensates on the surface³³.

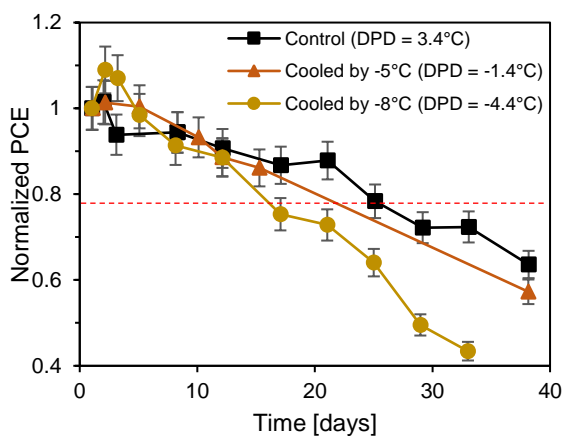
240 In order to only evaluate the effect of the dew point depression, the samples were kept horizontally,
 241 excluding the influence of inclination of the samples, which was different in each test site. The I-V
 242 measurements were done in situ and samples were monitored at constant conditions. Thus, the level of
 243 condensation on the modules was kept constant throughout the test, without evaporation and the
 244 samples were not subjected to temperature or humidity cycling.

245 Figure 11 shows the impact of cooling the modules during the ISOS-D-3 tests. Since the performance
 246 measurements were done in situ and not at the standard temperature, data was normalized to the first
 247 value. It is clear that the modules that were cooled the most, exhibited the greatest degradation. More
 248 condensation was formed on the module surface, providing confirmation that modules, when operated
 249 in Bangor, should exhibit faster degradation, induced by the reduction of FF and V_{oc} , with greater
 250 periods at lower DPD ranges.



251
 252 **Figure 10** - Samples under the indoor test. The climate chamber was set at 65 °C and 85 % RH and two samples
 253 were placed over a peltier and cooled by -5 and -8°C (test under -5°C being depicted). The formation of water drops
 254 on top of the samples is evidence of induced condensation.

255



256
 257 **Figure 11** – PCE of OPV modules tested under ISOS-D-3 conditions (65°C, 85% RH) with different levels of cooling
 258 applied to induce greater condensation on modules, which leads to different dew point depression (DPD) values.
 259 The red line identifies the points when T80 was reached. Error bars represent the standard deviation.

260 **4. CONCLUSION**

261
 262 The study showed that OPV modules fabricated with the same materials and processes can suffer
 263 different degradation when applied to different locations and seasons. In this case, modules fabricated
 264 at CSEM Brasil in the same coating run underwent a faster degradation when tested in Bangor, North
 265 Wales, compared to Belo Horizonte, Brazil. Different factors could have contributed to this, such as
 266 different light spectra and higher salinity in Bangor, but the main contribution was likely due to higher
 267 condensation in Bangor, based on the lower dew point depression showed by weather data and
 268 corroborated by an indoor test. The influence of condensation is poorly addressed in the literature about
 269 the stability of organic modules and raises the importance of carrying out more outdoor tests in different

270 climates and under real conditions to assess the most important stressors for each case. Based on this,
271 OPV materials and stacks could be optimized not only for specific applications, but also for different
272 locations, seeking the best performance with the longer lifetime. From this test, it was clear that in
273 environments such as Bangor, encapsulation is critical, and this problem could be addressed by the
274 use of high-performance barrier films or even the use of self-cleaning and hydrophobic coatings;
275 whereas in environments with high irradiance levels throughout the year, such as Belo Horizonte, a
276 search for more photostable materials is of paramount importance.

277

278 **SUPPLEMENTARY MATERIAL**

279

280 See supplementary material for the data of series and shunt resistance of the outdoor test.

281

282 **DATA AVAILABILITY STATEMENT**

283

284 The data that support the findings of this study are available from the corresponding author upon
285 reasonable request.

286

287 **REFERENCES**

288 ¹ R. Ilmi, A. Haque, and M.S. Khan, *Org. Electron. Physics, Mater. Appl.* **58**, 53 (2018).

289 ² L. Duan, N.K. Elumalai, Y. Zhang, and A. Uddin, *Sol. Energy Mater. Sol. Cells* **193**, 22 (2019).

290 ³ K. Gao, S.B. Jo, X. Shi, L. Nian, M. Zhang, Y. Kan, F. Lin, B. Kan, B. Xu, Q. Rong, L. Shui, F. Liu, X. Peng, G.
291 Zhou, Y. Cao, and A.K.Y. Jen, *Adv. Mater.* **31**, 1 (2019).

292 ⁴ H. Lee, C. Park, D.H. Sin, J.H. Park, and K. Cho, *Adv. Mater.* **30**, 1 (2018).

293 ⁵ Y. Cui, H. Yao, L. Hong, T. Zhang, Y. Xu, K. Xian, B. Gao, J. Qin, J. Zhang, Z. Wei, and J. Hou, *Adv. Mater.* **31**,
294 1 (2019).

295 ⁶ Q. Liu, Y. Jiang, K. Jin, J. Qin, J. Xu, W. Li, J. Xiong, J. Liu, Z. Xiao, K. Sun, S. Yang, X. Zhang, and L. Ding, *Sci.*
296 *Bull.* (2020).

297 ⁷ L. Meng, Y. Zhang, X. Wan, C. Li, X. Zhang, Y. Wang, X. Ke, Z. Xiao, L. Ding, R. Xia, H.L. Yip, Y. Cao, and Y.
298 Chen, *Science (80-.)*. **361**, 1094 (2018).

299 ⁸ C.J. Mulligan, C. Bilen, X. Zhou, W.J. Belcher, and P.C. Dastoor, *Sol. Energy Mater. Sol. Cells* **133**, 26 (2015).

300 ⁹ M.D. Chatzisideris, A. Laurent, G.C. Christoforidis, and F.C. Krebs, *Appl. Energy* **208**, 471 (2017).

301 ¹⁰ J. Yuan, Y. Zhang, L. Zhou, G. Zhang, H.L. Yip, T.K. Lau, X. Lu, C. Zhu, H. Peng, P.A. Johnson, M. Leclerc, Y.
302 Cao, J. Ulanski, Y. Li, and Y. Zou, *Joule* **3**, 1140 (2019).

303 ¹¹ Y. Cui, H. Yao, J. Zhang, T. Zhang, Y. Wang, L. Hong, K. Xian, B. Xu, S. Zhang, J. Peng, Z. Wei, F. Gao, and
304 J. Hou, *Nat. Commun.* **10**, 1 (2019).

305 ¹² Y. Zhang, I.D.W. Samuel, T. Wang, and D.G. Lidzey, *Adv. Sci.* **5**, (2018).

306 ¹³ Printed Electronics World, *Third Generation Solar Energy Used For the First Time in Brazil Mall* (2019).

307 ¹⁴ Printed Electronics World, *Greenhouses Fitted with Organic Photovoltaic Film* (2019).

- 308 ¹⁵ *Brazilian Co Sunew to Install World's Largest Organic PV System* (2019).
- 309 ¹⁶ OPE Journal, *World's Largest BiOPV Installation Completed in France Using Heliatek's Solar Film Solution*,
310 *HeliaSol* (2017).
- 311 ¹⁷ M.O. Reese, S.A. Gevorgyan, M. Jørgensen, E. Bundgaard, S.R. Kurtz, D.S. Ginley, D.C. Olson, M.T. Lloyd, P.
312 Morvillo, E.A. Katz, A. Elschner, O. Haillant, T.R. Currier, V. Shrotriya, M. Hermenau, M. Riede, K.R. Kirov, G.
313 Trimmel, T. Rath, O. Inganäs, F. Zhang, M. Andersson, K. Tvingstedt, M. Lira-Cantu, D. Laird, C. McGuinness, S.
314 Gowrisanker, M. Pannone, M. Xiao, J. Hauch, R. Steim, D.M. Delongchamp, R. Rösch, H. Hoppe, N. Espinosa,
315 A. Urbina, G. Yaman-Uzunoglu, J.B. Bonekamp, A.J.J.M. Van Breemen, C. Giroto, E. Voroshazi, and F.C. Krebs,
316 *Sol. Energy Mater. Sol. Cells* **95**, 1253 (2011).
- 317 ¹⁸ R. Roesch, T. Faber, E. Von Hauff, T.M. Brown, M. Lira-Cantu, and H. Hoppe, *Adv. Energy Mater.* **5**, 1 (2015).
- 318 ¹⁹ N. Grossiord, J.M. Kroon, R. Andriessen, and P.W.M. Blom, *Org. Electron. Physics, Mater. Appl.* **13**, 432
319 (2012).
- 320 ²⁰ S.A. Gevorgyan, I.M. Heckler, E. Bundgaard, M. Corazza, M. Hösel, R.R. Søndergaard, G.A. Dos Reis Benatto,
321 M. Jørgensen, and F.C. Krebs, *J. Phys. D. Appl. Phys.* **50**, (2017).
- 322 ²¹ P. Kumar, C. Bilen, B. Vaughan, X. Zhou, P.C. Dastoor, and W.J. Belcher, *Sol. Energy Mater. Sol. Cells* **149**,
323 179 (2016).
- 324 ²² P. Cheng and X. Zhan, *Chem. Soc. Rev.* **45**, 2544 (2016).
- 325 ²³ Y. Zhang, H. Yi, A. Iraqi, J. Kingsley, A. Buckley, T. Wang, and D.G. Lidzey, *Sci. Rep.* **7**, 1 (2017).
- 326 ²⁴ M. Corazza, F.C. Krebs, and S.A. Gevorgyan, *Sol. Energy Mater. Sol. Cells* **143**, 467 (2015).
- 327 ²⁵ J. Kettle, V. Stoichkov, D. Kumar, M. Corazza, S.A. Gevorgyan, and F.C. Krebs, *Sol. Energy Mater. Sol. Cells*
328 **167**, 53 (2017).
- 329 ²⁶ S.A. Gevorgyan, M. V. Madsen, H.F. Dam, M. Jørgensen, C.J. Fell, K.F. Anderson, B.C. Duck, A. Mescheloff,
330 E.A. Katz, A. Elschner, R. Roesch, H. Hoppe, M. Hermenau, M. Riede, and F.C. Krebs, *Sol. Energy Mater. Sol.*
331 *Cells* **116**, 187 (2013).
- 332 ²⁷ M.Z. Jacobson and V. Jadhav, *Sol. Energy* **169**, 55 (2018).
- 333 ²⁸ A. Distler, T. Sauermann, H.J. Egelhaaf, S. Rodman, D. Waller, K.S. Cheon, M. Lee, and D.M. Guldi, *Adv.*
334 *Energy Mater.* **4**, 1 (2014).
- 335 ²⁹ T. Heumueller, W.R. Mateker, A. Distler, U.F. Fritze, R. Cheacharoen, W.H. Nguyen, M. Biele, M. Salvador, M.
336 Von Delius, H.J. Egelhaaf, M.D. McGehee, and C.J. Brabec, *Energy Environ. Sci.* **9**, 247 (2016).
- 337 ³⁰ S.K. Gupta, K. Dharmalingam, L.S. Pali, S. Rastogi, A. Singh, and A. Garg, *Nanomater. Energy* **2**, 42 (2013).
- 338 ³¹ Sensirion, *Application Note, Dew-Point Calculation* (2006), pp. 1–3.
- 339 ³² O.A. Alduchov and R.E. Eskridge, *J. Appl. Meteorol.* **35**, 601 (1996).
- 340 ³³ J. Oshikiri and T.N. Anderson, in *23rd Int. Symp. Transp. Phenom.* (2012).
- 341